INTERNATIONAL JOURNAL OF SUSTAINABLE CONSTRUCTION ENGINEERING AND TECHNOLOGY
ISSN: 2180-3242 e-ISSN: 2600-7959

IJSCET

Vol. 16 No. 3 (2025) 87-104
https://publisher.uthm.edu.my/ojs/index.php/ijscet

Enhancing Concrete Performance with Fly Ash and Cellulose Nanocrystals: A Comprehensive Study

Varsha More Varsha[1]*, Surekha Bhalchandra[1], Sanjay Jamkar[1]

[1] *Government Engineering College, Chhatarpati Sambhajinagar, INDIA*

*Corresponding Author: varshatmore1@gmail.com
DOI: https://doi.org/10.30880/ijscet.2025.16.03.007

Article Info

Received: 21 February 2025
Accepted: 6 November 2025
Available online: 5 December 2025

Keywords

Sustainable concrete, fly ash, cellulose nanocrystal, mechanical properties, microstructural analysis, regression analysis

Abstract

The production of concrete is heavily dependent on cement, which plays a major role in environmental challenges like high carbon emissions. This research examines how incorporating fly ash (FA) and cellulose nanocrystals (CNC) affects the characteristics of concrete. FA partially replaced cement at 0-50%, while CNC was added at 0-1% by cement mass. The optimal mix (FA20CNC0.2) with 20% FA and 0.2% CNC showed significant improvements in mechanical properties compared to conventional concrete: 36.54% higher compressive strength, 19.94% higher split tensile strength, 18.22% higher flexural strength, and 21.21% higher shear strength. Regression models with high accuracy ($R^2 > 0.95$) were developed to predict secondary mechanical properties from compressive strength, streamlining the mix design process. SEM analysis revealed a denser microstructure with fewer microcracks in FA20CNC0.2. EDS indicated higher amounts of strength-enhancing components like $CaCO_3$ and SiO_2. The combined effect of FA and CNC boosted the pozzolanic reaction, refined the pores, and led to the formation of additional calcium-silicate-hydrate (C-S-H) gel. This approach reduces cement use while enhancing performance, offering an eco-friendly solution for sustainable high-performance concrete production.

1. Introduction

Sustainable concrete can be developed by incorporating waste materials from agricultural and industrial sources as partial replacements for cement. These waste by-products serve as supplementary cementitious materials (SCMs), which help reduce cement consumption and, consequently, carbon dioxide (CO_2) emissions in the construction sector [1]. Supplementary cementitious materials (SCMs) commonly used include fly ash (FA), ground-granulated blast-furnace slag (GGBFS), metakaolin (MK), rice husk ash (RHA), and silica fume (SF). Fly ash is the most prevalent owing to its wide availability [2], [3], [4], [5], [6], [7], [8].

Globally, millions of tons of fly ash are produced annually, and this trend is expected to continue [9]. In India alone, coal-fired power plants generate approximately 180 million metric tons of fly ash annually [10], posing a significant landfill management challenge. Incorporating this material into concrete not only tackles environmental issues but also enhances sustainability.

Understanding the environmental advantages of fly ash leads to a closer examination of its characteristics, as outlined by ASTM C618-23, which categorizes fly ash into Class C and Class F, with a lower calcium oxide (CaO) content, and exhibits a stronger pozzolanic reaction during hydration than Class C. The inclusion of fly ash in concrete has been shown to enhance the matrix properties and contribute to sustainable construction practices [11]. Studies have suggested that replacing up to 10% of cement with fly ash improves the workability

of fresh concrete and the strength of high-performance concrete [12], whereas a 20% replacement can positively influence the microstructure of mature concrete [13].

Although SCMs such as fly ash offer notable sustainability benefits, they also present challenges, such as reduced early age strength, increased drying shrinkage, and higher water absorption [14], [15]. Faced with these challenges, researchers have turned to innovative strategies, such as merging SCMs with nanotechnology, to boost the effectiveness of concrete. The integration of SCMs such as FA, SF, and MK with nanomaterials helps overcome the limitations of each material [16] , [17], [18], [19], [20] [21], [22], [23], [24]. Nanotechnology enables the synthesis and assembly of nanostructures through "top-down" and "bottom-up" approaches [25], [26]. Particles with sizes less than 200 nm are classified as nanomaterials, although a minimum particle size of 500 nm is typically required for effective integration into concrete [27]. Graphical comparisons of the specific surface areas and particle sizes of the SCMs and nanomaterials highlight these differences [28].

Among the various nanomaterials used in concrete, such as nano-silica [29], [30], [31]nano-titanium dioxide [32], and carbon nanotubes [33], increasing attention has been directed towards sustainable and renewable options. Investigating the potential of nanocellulose involves understanding its synergistic effects with FA in the concrete matrix to enhance sustainability and performance [34]. Owing to its eco-friendly nature, nanocellulose has been applied in various industries, such as food and cosmetics [35], and more recently, in cementitious materials [36], [37].

Nanocellulose exists in four main forms: cellulose nanocrystals (CNC), cellulose nanofibrils (CNF), bacterial cellulose (BC), and cellulose filaments (CF) [38] [39]. CNC are particularly valued because of their high tensile modulus and strength, low density, large surface area, and abundance of hydroxyl groups, which enhance the mechanical performance of cement matrices [40]. These characteristics render them effective as an environmentally sustainable reinforcing agent within the construction sector [41]. Their incorporation not only aligns with sustainable development goals but also significantly improves the mechanical and microstructural characteristics of cementitious composites. For example, [42] demonstrated that the addition of 0.2 wt% and 1 wt% CNCs to cement paste resulted in an increase in compressive strength by approximately 10% and 17%, respectively. Further the inclusion of 0.8 wt% wood-based CNCs led to a 20% enhancement in compressive strength after freeze-thaw cycles, along with a 60% reduction in carbonation depth [43]. This study [44] reported that inclusion of CNC led to increases in compressive strength (18.8–22.14%), splitting tensile strength (19.4–26.38%), and flexural strength (32–44.67%) in mixtures with water-to-cement ratios of 0.3 and 0.5. These findings collectively contribute to a deeper understanding of the bond behavior and performance of CNC-enhanced concrete materials.

The effective dosage of cellulose nanocrystals (CNCs) varies depending on both the source material and the type of cement with which they are combined. In the present study, CNCs extracted from cotton seed balls were incorporated into mixtures containing Ordinary Portland Cement (OPC). A review of existing literature [38] indicates that CNCs are typically used within a range of 0.1% to 1% by weight of cement, higher dosages can lead to adverse effects on both the fresh and hardened properties of cementitious materials. For instance, [44] reported that while CNC additions up to 1 wt% enhanced compressive strength and refined the microstructure of cement pastes, dosages beyond this level resulted in agglomeration and poor dispersion, leading to decreased mechanical performance. Similarly, [42] found that excess CNC increased the viscosity of the cement paste, reduced workability, and hindered hydration by blocking capillary pores, negatively affecting strength development. Furthermore, [43] emphasized that an optimal CNC content exists, beyond which no significant improvement is observed and, in some cases, performance deterioration occurs due to non-uniform distribution and excessive water demand. Therefore, based on these findings, a dosage range of 0–1 wt% is considered optimal for CNC incorporation.

This study examined the synergistic application of FA and CNC to overcome the limitations associated with SCMs. While FA promotes sustainability by reducing the amount of cement required, CNC enhances the concrete matrix's strength and durability by filling micropores and encouraging the formation of additional calcium silicate hydrate (C-S-H) gels. Based on previous studies [45], [46], cement was partially replaced with FA in increments of 10%, ranging from 0% to 50%. However, the current Indian Standards (IS 456:2000) do not specify dosage limits for FA, emphasizing only the need for uniform mixing [47].

The optimal proportions of FA and CNC were experimentally determined by evaluating the compressive strength of standard concrete mixes. The optimized mixtures were subsequently employed to evaluate essential mechanical characteristics, such as compressive, split tensile, flexural, and shear strengths, in addition to conducting microstructural analysis through Energy Dispersive X-ray Spectroscopy (EDS). The results were correlated with those of conventional and FA-only concrete to evaluate the effectiveness of the combined FA-CNC system in enhancing concrete performance. A regression analysis was conducted on concrete modified with FA–CNC to identify the empirical relationships between mechanical properties.

2. Experimental Program

2.1 Raw Material

2.1.1 Cement

Ordinary Portland cement (OPC-53) was used for casting with a standard consistency of 28.5, Blain's fineness of 329 m^2/kg, and density of 3.14 g/cc, as per the requirements of IS 269:2015 [48]. Table 1 displays the chemical constituents of the cement.

2.1.2 FA

The processed FA used in the study was procured from Dirk India Pvt. Ltd. from the Nashik region named Pozzocrete 100 as per IS 3812 (Part-1): 2013 specification [49]. The specific surface fineness obtained by Blain's permeability method (Min) was 640 m^2/kg, and the lime reactivity was 9.3 N/mm^2. The chemical constituents of FA is depicted in Table 1.

Table 1 *Chemical constituents of OPC and FA*

Constituents wt %	CaO	SiO_2	Al_2O_3	Fe_2O_3	Na_2O	SO_3	MgO	Cl	LOI
OPC 53	70.85	17.20	2.87	3.10	0.36	2.42	1.23	0.015	1.92
FA	2.14	58.24	29.37	5.53	0.45	0.52	1.58	0.021	0.72

2.1.3 CNC and Dispersion Method

The CNC utilized in this research, featuring a specific surface area of 1.4 m^2/g, was sourced from Vedayukt India Pvt. Ltd. in Jharkhand. Extracted from raw cotton seeds through a combination of acid hydrolysis methods, the CNC appeared as a milky white powder, as depicted in Fig. 1a. The Suspension is shown in Fig. 1b. The uniform dispersion of the nanomaterial in the mix was the primary challenge to be used in the mix. Some studies have replicated the improvement in flexural strength by approximately 20-30% using CNC treated with the ultrasonic dispersion method [50]. CNC was dispersed equally with magnetic stirring and ultrasonic dispersion to improve the distribution of particles within the mixture, and a zeta potential of 40 mV was also more stable [43], [51].

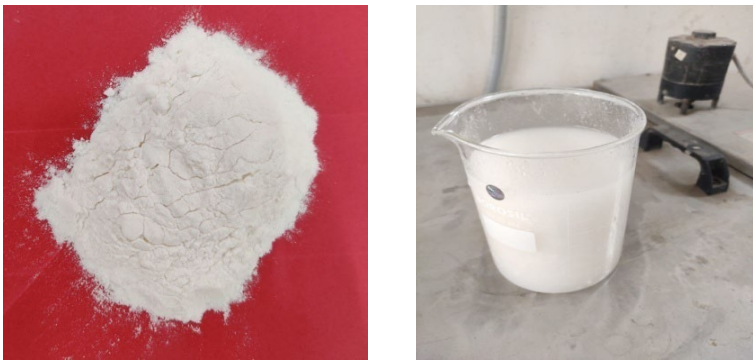

(a) CNC Powder form **(b) Suspension form**

Fig. 1 *(a) CNC powder form; (b) Suspension form*

Hence, to overcome the issue of dispersibility, the CNC was treated with magnetic stirring and ultrasonication to achieve better performance. Table 2 displays the CNC's physical and chemical characteristics.

Table 2 *The physical and chemical properties of CNC*

Molecular Formula	Crystallite density	Form	Specific surface area	Average particle length	pH	Particle Diameter	Purity
$(C_6H_{10}O_5)_n$	1.60 g/cm^3	Milky white	1.40 m^2/g	200nm	5.5-7.5	<100nm	99%

The compactness of concrete is influenced by the distribution of its pore sizes. When these two materials are combined, they form a more compact structure that improves both mechanical strength and durability. The

particle size distribution was analyzed using the circular equivalent diameter – Number Distribution graphs shown in Fig. 2, which allowed for the assessment of particle fineness. The analysis was conducted using equipment from Malvern Panalytical Ltd. According to the graph, fly ash exhibited a smaller median particle size of 4.37 µm, whereas the cement particles ranged from approximately 6 to 10 µm. This indicates that fly ash is finer and more uniform than cement, which can influence key properties such as hydration, initial setting time, and homogeneous mixing in cementitious materials.

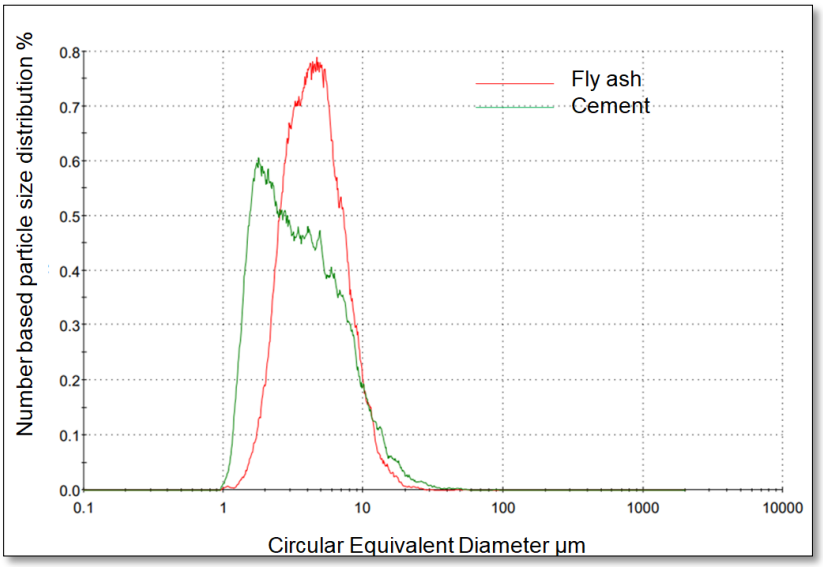

Fig. 2 *Particle size distribution: fly ash and cement*

Fig. 3 illustrates the distribution of particle sizes, indicating that the diameter of the particles was under 100 nm. The CNC helped fill the fine pore gaps, resulting in a denser concrete matrix.

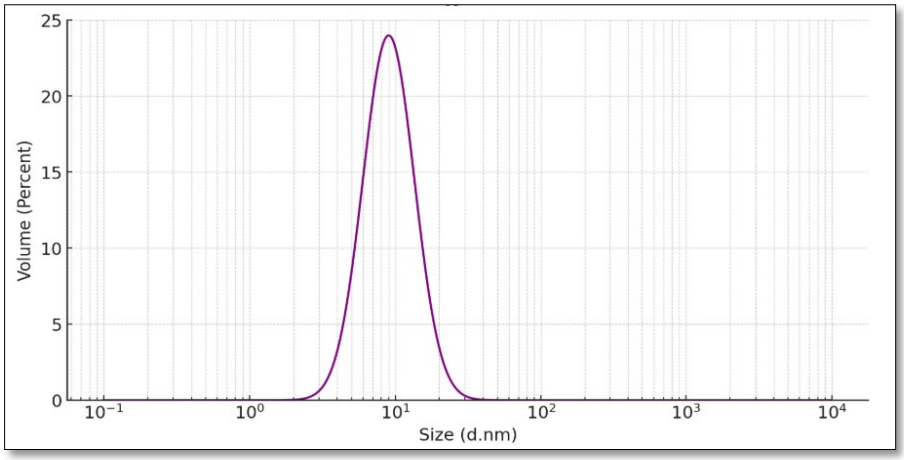

Fig. 3 *Particle size distribution of CNC*

2.1.4 Coarse Aggregate, Fine Aggregate, and Crushed Sand

Coarse aggregates measuring 12.5 mm with a specific gravity of 2.95 and a fineness modulus of 3.28, as well as aggregates sized at 20 mm with a specific gravity of 2.96 and a fineness modulus of 3, were utilized. In accordance with IS 383:2016, crushed sand was used with a specific gravity of 2.78 and a fineness modulus of 3.05 [52].

Int. J. of Sustainable Construction Engineering and Tech. Vol. 16 No. 3 (2025) p. 87-104

2.1.5 Superplasticizer and Water

The superplasticizer of Asian paints-Technoplast S300 was used in the mixture. The liquid exhibited a brown hue, possessing a relative density of 1.165 and maintaining a pH of 7.62 at 25°C. Tap water, free of organic matter, was used for casting.

2.2 Mix Proportion of Concrete in (kg/m^3)

The concrete mix design was performed according to IS 10262:2019 guidelines [53]. The mixing combinations of the FA, CNC, crushed sand, coarse aggregate, fine aggregate, water, and superplasticizer used in this study are shown in Table 3, where the following notations were used to show the mixing combination for CNC Mix proportion: CC- Conventional concrete mix without considering CNC and FA, CNC0.1 to CNC1 at the interval of 0.1%, CNC added in concrete mix by mass of cement, and FA Mix proportion FA10, FA20, FA30, FA40, and FA50 - mix with replacement of cement by 10, 20, 30, 40, and 50% FA by mass of cement. In the case of the Combined FA and CNC, the designation FA20CNC0.2 signifies that 20% of the cement is substituted with FA, and 0.2% CNC is added by the cement's mass, representing the optimal proportions of CNC and FA.

The optimized percentages of FA and CNC were combined, as experimental findings indicated that adding more CNC led to a decrease in compressive strength. Similarly, replacing FA with more than 20% also leads to diminished compressive strength, as demonstrated experimentally. Based on these findings, the FA20CNC0.2 concrete mix was finalized without further CNC or FA replacements. FA20CNC0.2 signifies that 20% of the cement's mass is substituted with FA, and an additional 0.2% CNC is added, also based on the cement mass. The FA-based combination, which is widely used in practical applications, served as a reference point for evaluating the mechanical properties. The FA20CNC0.2 mixture was assessed in comparison to FA-based concrete and traditional concrete to emphasize the effects of combining FA and CNC on both mechanical performance and microstructural characteristics.

Table 3 *Mixing proportions in kg/m^3*

Mix	Cement	FA	Crushed Sand	Fine aggregate 10mm	Course Aggregate 12mm	Water	CNC Additive in % of cement	CNC Additive	W/C ratio	SP
CNC Mix proportion										
CC	400	-	858	360	770	155	0	0	0.39	0.6
CNC 0.1	400	-	858	360	770	155	0.1	0.4	0.39	0.6
CNC 0.2	400	-	858	360	770	155	0.2	0.8	0.39	0.6
CNC 0.3	400	-	858	360	770	155	0.3	1.2	0.39	0.6
CNC 0.4	400	-	858	360	770	155	0.4	1.6	0.39	0.6
CNC 0.5	400	-	858	360	770	155	0.5	2.0	0.39	0.6
CNC 0.6	400	-	858	360	770	155	0.6	2.4	0.39	0.6
CNC 0.7	400	-	858	360	770	155	0.7	2.8	0.39	0.6
CNC 0.8	400	-	858	360	770	155	0.8	3.2	0.39	0.6
CNC 0.9	400	-	858	360	770	155	0.9	3.6	0.39	0.6
CNC 1	400	-	858	360	770	155	1	4	0.39	0.6
FA Mix proportion										
FA10	360	40	858	360	770	155	-	-	0.39	0.6
FA20	320	80	858	360	770	155	-	-	0.39	0.6
FA30	280	120	858	360	770	155	-	-	0.39	0.6
FA40	240	160	858	360	770	155	-	-	0.39	0.6
FA50	200	200	858	360	770	155	-	-	0.39	0.6
Combined FA and CNC										
FA 20CNC0.2	320	80	858	360	770	155	0.2	0.8	0.39	0.6

The water-to-cement ratio was kept at 0.39. Initially, all dry components, including coarse and fine aggregates, crushed sand, cement, and FA, were thoroughly mixed for 2 minutes using a pan mixer. Meanwhile, the specified amount of CNC was mixed with 600 ml of water, which was magnetically stirred for 4 min, and ultrasonication was performed at two intervals for 16 min. The dispersed suspension was mixed with the estimated amount of water and a specified quantity of superplasticizer. The solution was mixed thoroughly with the dry ingredients for 3 min. and was used to obtain a homogeneous mixture of the sample. The molds were filled with a mixture that was subjected to vibration to ensure a dense structure. Subsequently, the molds were left to cure for a period of 24 hours at a consistent temperature of 24°C. Subsequently, the cubes were removed from the molds and allowed to cure at room temperature for 28 days in accordance with the provisions of IS 516:1959 [54], as shown in Fig. 4.

Fig. 4 *Casting of concrete cubes*

2.3 Experimental Methods

2.3.1 Mechanical Properties Tests

Concrete cubes with dimensions of 150 mm were cast to assess the compressive strength at 7 and 28 days, following the IS 456:2000 specifications [47] for CNC and FA mix proportions. Following a 28-day curing period, the combined mixture underwent tests to assess its flexural strength, shear strength, and split tensile strength, in addition to a microstructural examination using energy-dispersive X-ray spectroscopy (EDS). For the split tensile strength test, cylindrical specimens with a diameter of 100 mm and height of 200 mm were prepared according to IS 5816:1999 [55]. The flexural strength was determined using prisms with a cross-sectional area of 100 mm × 100 mm and a length of 500 mm, following the procedures outlined in IS 516:1959 [45].

As no standardized method exists for the direct measurement of shear strength in concrete matrices, the established literature [56] was used to define the testing protocol. Standard 150 mm concrete cubes were used for the shear strength evaluation. To ensure the reliability of the mechanical tests, the average results from three samples were recorded. The tests were performed using a compression testing machine with a 200-ton capacity from EIE Instruments Pvt. Ltd., which was routinely calibrated to guarantee precise measurements.

To explore the combined impact of CNC and FA within the cement matrix after a 28-day curing period, a microstructural examination was performed alongside EDS. The concrete powder, sourced from the crushed samples that demonstrated the greatest compressive strength, was scrutinized using a JEOL JSM-6510 scanning electron microscope, which was fitted with an Oxford Instruments EDS (EDAX) system. SEM imaging was performed at a consistent magnification of 7500×, with all images captured at a 2 μm scale to facilitate direct comparisons across samples. Six images per mix were captured, and the highest-quality micrographs were selected for analysis. The selected images were appropriately labelled[P2] to highlight specific microstructural features relevant to CNC and FA interactions.

Figure 5 provides a depiction of the experimental setup and specimen specifics, while Figure 6a illustrates the SEM configuration. The processes for sample conditioning and positioning are depicted in Figures 6b and 6c, respectively.

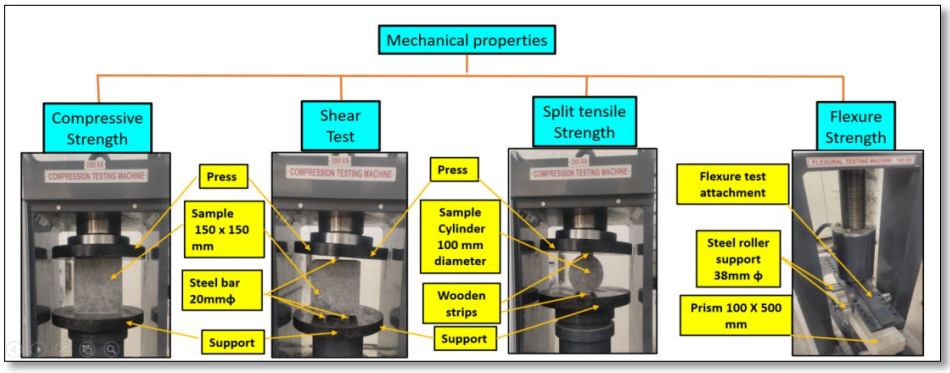

Fig. 5 *Mechanical properties testing equipment with samples*

(a) SEM Equipment **(b) Sample Conditioning** **(c) Sample positioning**

Fig. 6 *Scanning electron microscopy equipment with samples*

3. Result and Discussion

3.1 Compressive Strength of CNC and FA Mix Proportions

The compressive strength test results for the CNC and FA mix proportions at 7 and 28 d are shown in Fig. 7 and 8, respectively. From the graph, the optimum percentage was determined and considered for the combined mix proportion experiment.

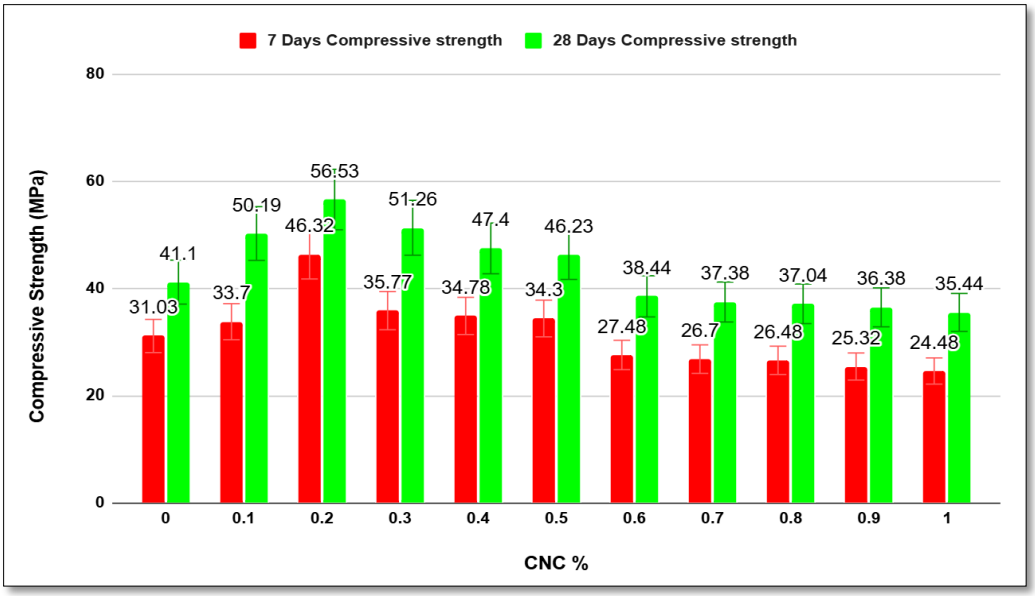

Fig. 7 *Compressive strength of CNC*

Figure 7 illustrates that incorporating CNC into the concrete matrix led to a notable enhancement. The concrete mix with a 0.2% CNC addition achieved the highest strength among all the variations. Strength increased with CNC additions of 0.1%, 0.2%, and 0.3% by cement mass, compared to CC, over a 28-day

compressive strength period. However, further addition of CNC beyond this point led to a decrease in strength owing to the agglomeration effect [38], [57]. The incorporation of CNC at 0.1, 0.2, 0.3, 0.4, and 0.5% increased the strength by 22.12%, 37.54%, 24.72%, 15.32%, and 12.48%, respectively, and further addition at 0.6, 0.7, 0.8, 0.9, and 1% decreased the strength by 6.47%, 9.05%, 9.88%, 11.48%, and 13.77%, respectively. Incorporating CNC at 0.2% of the cement mass led to a 37.54% increase in strength compared to the concrete matrix CC. Consequently, this proportion of CNC was selected for the combined mix proportion experiments.

Owing to its distinct characteristics, CNC plays a role in refining pores and densifying the matrix, which greatly boosts the concrete's compressive strength. The nanometric dimensions and extensive surface area of CNC allow it to serve as a nucleation site for the formation of hydration products, especially calcium-silicate-hydrate (C-S-H), resulting in a more compact microstructure. Additionally, the hydrophilic hydroxyl groups on the CNC surface interact with cement hydration products, enhancing the bonding within the matrix.

This improvement in mechanical properties aligns with results from earlier research. For example, [44]noted a 17% rise in compressive strength by adding 1 wt% CNC to cement paste, crediting the enhancement to better hydration kinetics and microstructural refinement. Likewise, [43] found an approximate 20% increase in compressive strength with 0.8 wt% CNC, even after undergoing durability tests like freeze-thaw cycles, highlighting the long-term advantages of CNC in cementitious composites.

In this study, a 0.2% CNC dosage resulted in a 37.54% increase in compressive strength, exceeding many previously reported figures. This improvement can be linked to the CNC source (cotton seed balls), its particle shape, and its synergistic interaction with the cement hydration process, which collectively form a more refined and continuous C-S-H gel network. However, when CNC content exceeds 0.3%, agglomeration effects become predominant, diminishing dispersion quality and creating stress-concentration zones, which ultimately lead to a reduction in strength.

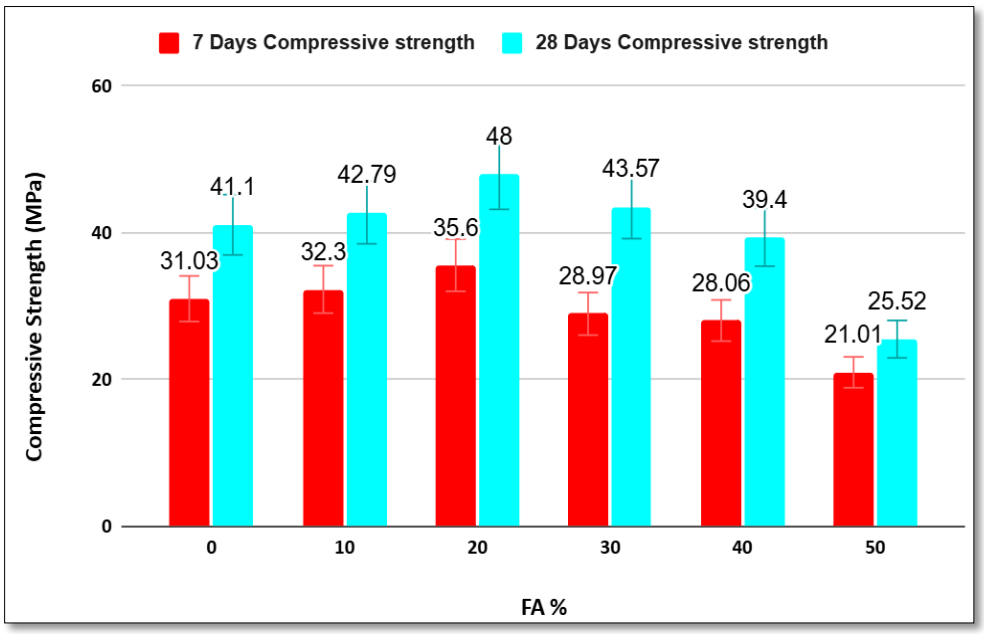

Fig. 8 *Compressive strength of FA*

The compressive strength performance with the replacement of FA at 0, 10, 20, 30, 40, and 50% by mass of cement is shown in Fig. 8. The graph shows an increase in the compressive strength with the replacement of FA by cement mass up to 20%. Further additions typically decrease the strength, primarily because the slow hydration process results in low early strength [58]. The replacement of FA at 10%, 20%, and 30% increases the strength by 4.11%, 16.78%, and 6%, and further replacement at 40% and 50% decreases the compressive strength by 4.13% and 37.90%, respectively. It was noted that replacing 20% FA by the FA mass with cement resulted in maximum strength.

The experimental study referenced in [59] indicates that using about 20% fly ash yields the best compressive strength in concrete mixtures, attributed to improved particle packing and pozzolanic reactions. This research [60] corroborates the beneficial filling effect and pozzolanic activity of approximately 20% fly ash replacement in UHPC, leading to enhanced strength performance. Further studies [61] have shown that a 20% fly ash replacement in UHPC improves both compressive and flexural strength, supporting the optimal range for strength performance. A 20% FA replacement was chosen based on experimental findings and alignment with

recent literature, as this amount optimally boosts compressive strength through better particle packing and pozzolanic activity, without significantly delaying early hydration.

3.2 Compressive Strength and Split Tensile Strength of Combined Mix Proportions

The compressive and split tensile strengths of FA20CNC0.2 after a curing period of 28 days, alongside a comparison with traditional concrete and an FA-based concrete matrix is shown in Figure 9.

The test results confirmed that the use of CNC and FA together in a cement matrix provided maximum compressive and split tensile strengths compared with conventional concrete. The performance was enhanced with the replacement of FA; additionally, the addition of CNC promoted more strength by making the concrete denser owing to its low density and high specific surface area. The concrete mixes FA20CNC0.2 and FA20 increased the compressive strength by 36.54% and 15.94%, respectively, compared with that ofth to CC. The maximum strength was obtained when 20% FA and 0.2% CNC were used by the mass of cement. Therefore, the carbon footprint can be effectively reduced with the combined use of FA and CNC by replacing 20% of cement. Additionally, the split tensile strengths of FA20CNC0.2 and FA20 were 19.94% and 5.89%, respectively, relative to those of CC. Therefore, the combined use of FA and CNC can be effective in improving the compression and split tensile strengths.

CNC plays an important role in enhancing concrete strength because of its finer size, as it fills the minute pores that remain in the matrix due to FA. CNC were attached to cement particles via a short-circuit diffusion process to enhance the strength parameters. The diffusion of water along the CNC enhanced the hydration of the unhydrated region, resulting in the formation of additional C-S-H bonds [62]. The hydrophilic nature of CNC also contributes to the hydration process, thereby increasing the number of C-S-H bonds and resulting in greater compressive strength [63], [64].

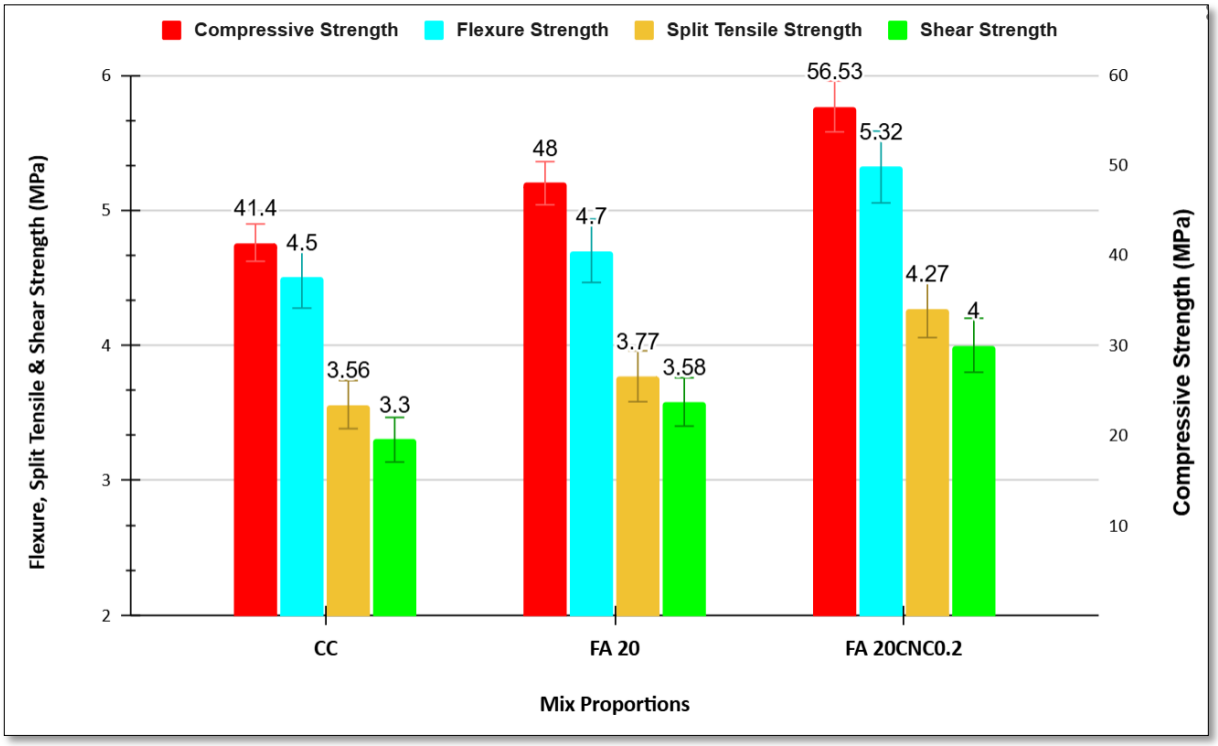

Fig. 9 *Compressive strength, flexure strength, split tensile strength and shear strength*

3.3 Flexural Strength

CNC and FA had a considerable impact on flexural strength, as depicted in Fig. 9. Compared with conventional concrete, all other mixes exhibited superior flexural strength.

The concrete matrix FA20CNC0.2 exhibited the greatest improvement compared with the other mixes. Using FA in conjunction with CNC was consistently advantageous, as the FA20CNC0.2 mixture exhibited a significant enhancement in flexural strength when compared to both traditional concrete and concrete based on FA. The flexural strength of the concrete matrices FA20CNC0.2 and FA20 was enhanced by 18.22% and 4.44%, respectively. The flexural strength of FA20CNC0.2 was 18.22%, making it the most preferable mix for flexural performance improvement.

The intricate pore structure of concrete boosts its flexural capabilities due to the smaller size, reduced density, and increased specific surface area of CNC. FA, abundant in silica, interacts with the high hydrogen content of CNC to create additional C-S-H bonds, leading to a more compact concrete structure. The joint application of CNC and FA lowered the water requirement, as CNC acted like superplasticizers, offering moderate workability and strength. This resulted in a decreased water-cement ratio, which enhanced the flexural strength of the CNC. Furthermore, the use of CNC with FA is advantageous because calcium and silicate ions are absorbed by CNC, stimulating the formation of C-S-H gel on its surface [65] .

3.4 Shear Strength

Figure 9 illustrates the shear strength of the FA20CNC0.2 mix in comparison to traditional concrete, as well as the FA-based concrete matrix that was cured for 28 days. The shear strength was determined by taking half of the maximum load at which the specimen failed and dividing it by the area of the cracked surface [56], as follows: The shear strengths of FA20CNC0.2 and FA20 were higher than that of CC. The tests were performed on three samples per concrete mixture. The shear performance was enhanced by 21.21% and 8.48% for the FA20CNC0.2 and FA20 concrete mixes, respectively.

The mechanical properties of concrete are improved through the combined use of FA and CNC, where FA acts as a lubricant and CNC enhances its mechanical strength [66]. The mechanism of cement cohesion significantly contributes to shear resistance. The properties of cement paste can be significantly influenced by the addition of cellulose nanocrystals (CNCs), which affect its cohesion through various mechanisms [67]. CNCs serve as rheology modifiers and improve the mechanical properties, playing an essential role in preserving the structural integrity and cohesion of the cement paste [68]. CNCs enhance the hydration reactions of cement, which are crucial for cohesion and strength development [65]. Cellulose nanocrystals (CNCs) can form channels within hydration products, enabling water transport and promoting the hydration of inner unhydrated cement particles. Enhanced cement hydration can positively affect compressive strength [38]. This enhanced compressive strength considerably increases the shear resistance. Figure 10 illustrates the shear failure patterns observed in the concrete cubes.

Fig. 10 *Shear failure pattern of cubes*

3.5 Regression-Based Modeling

Regression analysis was employed to establish empirical relationships between the compressive strength and other mechanical properties, including the split tensile, flexural, and shear strengths, of the FA-CNC-modified concrete. The resulting models exhibited high coefficients of determination (R^2), indicating strong predictive capability. These correlations enable the estimation of secondary strength parameters based on compressive strength alone, thereby minimizing the experimental effort while improving the efficiency of the mix design and quality assessment. Moreover, the derived equations offer a quantitative foundation for the structural modeling and lifecycle performance prediction of sustainable concrete. The following linear regression equations were formulated based on the experimental data: Equation 1 illustrates how split tensile strength is related to compressive strength, while Equation 2 outlines the link between flexural strength and compressive strength. Equation 3, on the other hand, specifies the association between shear strength and compressive strength. In these equations, STS stands for split tensile strength, FS signifies flexural strength, SS represents shear strength, and CS indicates compressive strength.

$$STS = 0.0475 \times CS + 1.557 \quad \text{Equation (1)}$$

$$FS = 0.0551 \times CS + 2.161 \quad \text{Equation (2)}$$

$$SS = 0.0464 \times CS + 1.369 \quad \text{Equation (3)}$$

These equations provide a robust framework for predicting the various strength parameters of FA-CNC-modified concrete based on compressive strength measurements. Figure 11 depicts the relationship between compressive strength and mechanical properties. A strong positive linear correlation was observed in all cases, as indicated by the high coefficient of determination (R^2) values.

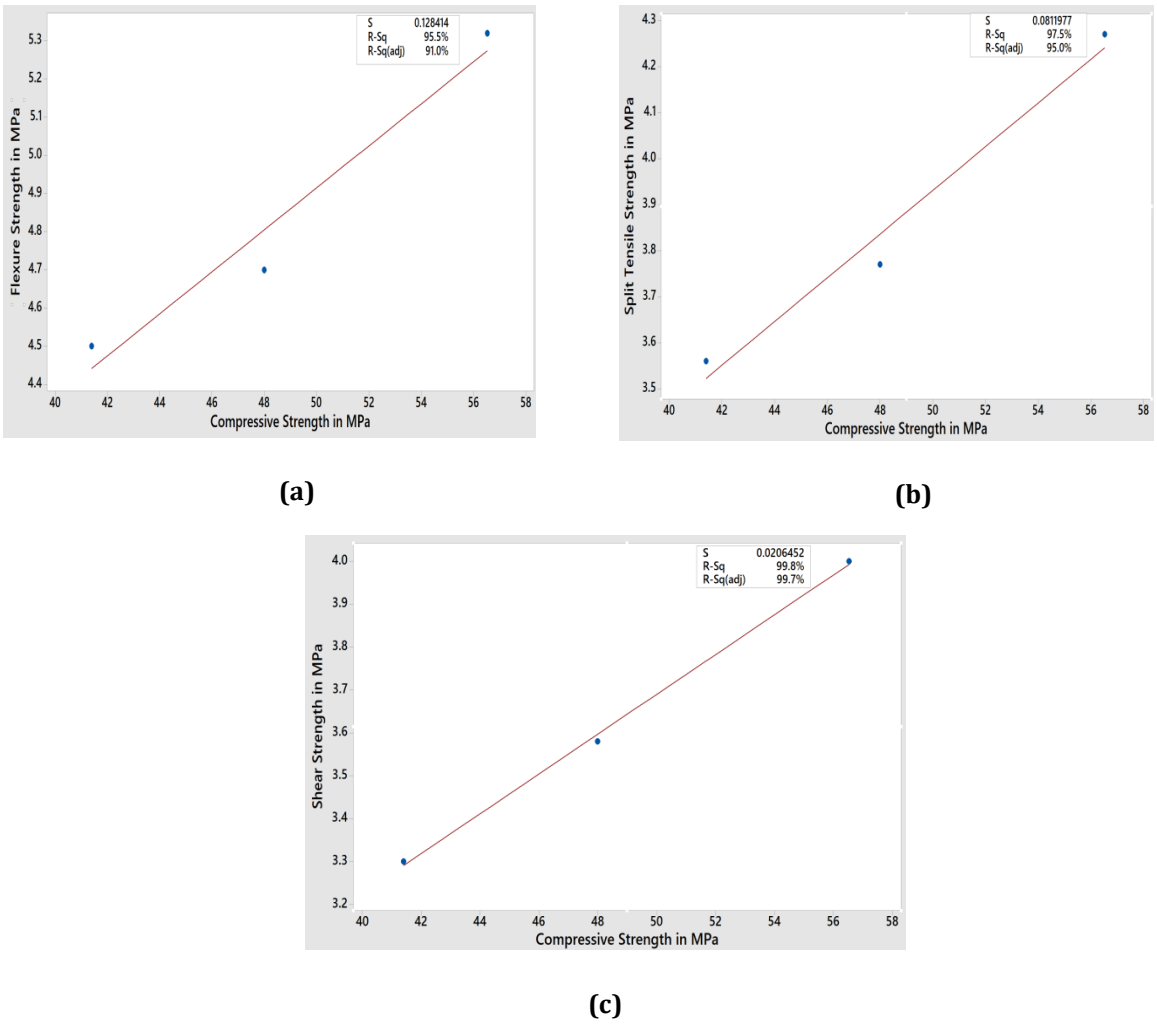

Fig. 11 *Correlation between (a) Compressive strength vs flexure strength; (b) Compressive strength vs split tensile strength; (c) Compressive strength vs shear strength*

Figure 11(a) illustrates that as the compressive strength rises, the flexural strength also increases in a proportional manner. The linear regression analysis produced an R^2 value of 95.5% and an adjusted R^2 value of 91.0%, demonstrating an excellent correlation between these two parameters. The flexural strength varied between 4.45 MPa and 5.30 MPa, corresponding to compressive strengths ranging from approximately 41 MPa to 57 MPa.

Figure 11(b) illustrates the connection between split tensile strength and compressive strength. A notably strong correlation was observed, with R^2 and adjusted R^2 values reaching 97.5% and 95.0%, respectively. As the compressive strength increased within the range of approximately 41–57 MPa, the split tensile strength varied from 3.50 MPa to 4.25 MPa.

The consistently high R^2 values across all mechanical properties suggest that the compressive strength serves as a reliable predictor of the flexural, split tensile, and shear strengths of concrete incorporating CNC and

FA. Minor deviations from the regression line were observed but remained within acceptable limits, as indicated by the low standard error (S) values shown in Fig. 11.

3.6 SEM and EDS analysis

The pore size distribution of the concrete mix was verified using SEM analysis to understand the enhancement parameters of its mechanical properties. The microscopic properties of the investigated concrete mix were significantly affected, which enhanced the mechanical properties to a higher level.

For every mix, SEM micro-images at 2µm and 7500 times magnification were taken for three samples, as depicted in Fig. 12 a), b), and c). Each image was labelled neatly to understand the variation in the microstructure of the concrete matrix cast by the application of CNC and FA.

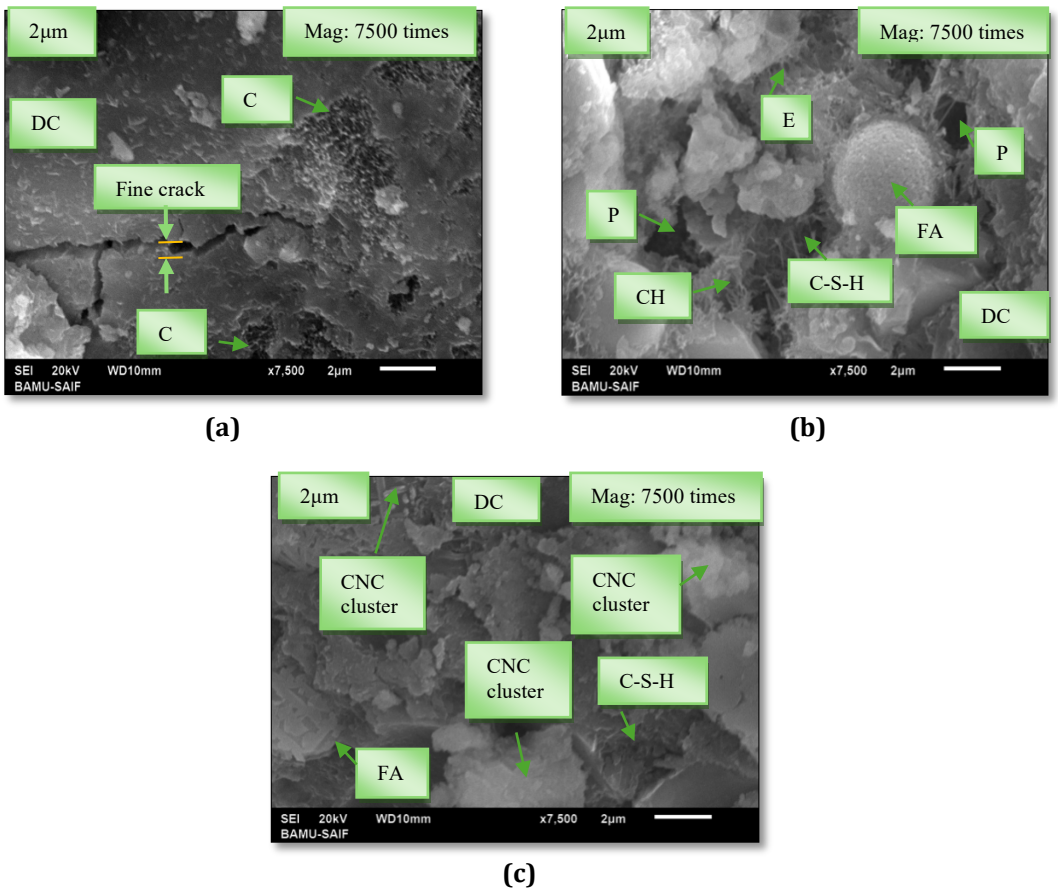

Fig. 12 *SEM images of (a) CC; (b) FA; (c) FA20CNC0.2*

Fig 12 (a) presents SEM images of conventional concrete that has been cured for 28 days. The majority of the image depicts the formation of a fully developed C-S-H gel stage. In some areas, the C-S-H appeared in a fibrous form with weak connections. The CH phase, encircled by the C-S-H phase, was also visible in the samples. Fine cracks were noted in the conventional concrete image due to the weak bonds among the surrounding binding materials. Additionally, small voids were detected in the concrete mix.

In the concrete matrix, a large amount of dense concrete matter (DCM) was clearly visible. The pozzocrete 100 material was well homogenized in the mix as the CNC adhered to the cement particles and created a path to enter the water, which increased the hydration process, resulting in the formation of more Calcium Silicate Hydrate (C-S-H) bonds [62]. The dense structure matrix was clearly visible owing to the combination of two finely graded SCMs and nanocellulose. The modified concrete matrix exhibited strong mechanical properties and a dense morphology.

EDS analysis was performed using SEM to study the composition of the concrete responsible for the formation of the cementitious phase and microstructure improvement. Table 4 shows the EDS analysis results for all the mixes.

Concrete with the incorporation of SCMs FA, the concrete matrix was modified slightly compared to that of CC. The concrete matrix modified with FA appeared homogeneous and dense in smaller amounts, as depicted in Fig. 12 (b). The SEM images of concrete samples containing FA showed that the voids were reduced to a some

degree and promoted the formation of C-S-H gel for improved strength properties. The rounded shape of FA was clearly visible with the C-S-H bond. In this concrete matrix, some microcracks along with the CH phase and porous area (P) filled with ettringite (E) were visible. The concrete area with weak bonds is indicated by a dotted blue line. However, a small amount of the CH phase was available compared to CC.

The concrete morphology of the mixes with CNC and FA changed significantly compared that with of the CC- and FA-based concrete, as shown in Fig. 12 (c). The concrete matrix was denser and more homogeneous when CNC and FA were considered. The maximum improvement was observed in the concrete mix FA20CNC0.2, as FA and CNC promoted the growth of CH to more C-S-H gel, which was responsible for the dense and strong structure of the concrete.

Table 4 *EDS analysis of all the mixes*

Compounds	CC	FA 20	FA20CNC0.2
SiO_2	49.58	47.55	51.23
Al_2O_3	2.94	3.67	3.79
MgO	1.34	1.21	2.39
$CaCO_3$	4.22	-	6.87
FeS_2	0.68	0.58	0.49
Elements	CC	FA 20	FA20CNC0.2
Ca	26.88	29.52	19.28
Si	10.55	11	10.99
Fe K	2.91	6.06	2.36
Na	0.43	-	-
K	-	0.39	-
Ti	0.46	-	0.44
Zr	-	-	2.15

The results indicated that calcium carbonate ($CaCO_3$), silicon dioxide (SiO_2), magnesium oxide (MgO), aluminum oxide (Al_2O_3), iron sulfide (FeS_2), and calcium (Ca) were present in the highest amounts compared to CC and FA20. In contrast, elements such as titanium (Ti), iron (Fe), potassium (K), and zirconium (Zr) were found in lower quantities than in CC and FA20CNC0.2. The significant presence of $CaCO_3$ contributes to the densification of the concrete phase, accelerates hydration, and enhances its mechanical strength [69], [70].

Because the CC and FA20 concrete mixes were already rich in SiO_2, they naturally exhibited a high SiO_2 content. This promotes the formation of calcium silicate hydrate (C-S-H) by reacting with calcium hydroxide ($Ca(OH)_2$), ultimately enhancing both the compressive and tensile strengths [71]. The replacement of FA and incorporation of CNC further increased the SiO_2 content, leading to greater strength development. Additionally, when the MgO content within the clinker was maintained between 2.0% and 5.0%, the cement strength improved and the setting time shortened. However, if the MgO level reaches approximately 8.0%, the cement strength slightly declines, and the setting time is extended [72]. FA20CNC0.2 contains MgO at 2.39%, which falls within the permissible range.

Furthermore, Al_2O_3 plays a crucial role in enhancing the compressive strength, reducing the porosity, and improving the durability by forming additional C-S-H and alumino-silicate hydrate phases [73]. The presence of FeS_2 can lead to sulfate ion formation, which, in the presence of water, reacts with cement matrix components to produce expansive products, ultimately causing cracks [74]. FA20CNC0.2 contains a minimal amount of FeS_2, which enhances its mechanical properties. Additionally, Ca contributes to the formation of dicalcium silicate and tricalcium silicate, which strengthen concrete through major C-S-H formation.

In conclusion, the combined FA20CNC0.2 mix enhanced the composition of the concrete phase, which was responsible for the improved mechanical properties.

Most importantly, the consumption of OPC was minimized as much as possible with the use of FA in the matrix with CNC to enhance the properties of concrete. This leads to a decrease in the production demand for cement, ultimately reducing CO2 emissions. The option proposed in this study satisfies these requirements.

The modified concrete matrix provides an eco-friendly solution, as more FA is used, minimum burden on open landfills, and organic nanocellulose (CNC) material is more suitable for sustainable, cost-effective, and denser concrete applications with higher mechanical properties.

4. Conclusion

Eco-friendly concrete can be produced using a combination of FA and CNC. These materials must be used at optimized percentages to achieve stronger concrete. The conclusions were derived from the experimental findings.

1. Incorporating both fly ash (FA) and cellulose nanocrystals (CNC) into concrete markedly improved its mechanical characteristics and microstructure when compared to traditional concrete and concrete made with only FA.
2. The optimum dosages were determined to be 20% FA replacement and 0.2% CNC addition by mass of cement (FA20CNC0.2).
3. The FA20CNC0.2 mix exhibited marked improvements in compressive strength (36.54% increase), split tensile strength (19.94% increase), flexural strength (18.22% increase), and shear strength (21.21% increase).
4. Regression analysis revealed strong relationships between the compressive strength and other mechanical properties of concrete modified with FA-CNC.
5. SEM analysis revealed a denser and more homogeneous microstructure in the FA20CNC0.2 mix, with fewer microcracks and voids than in conventional concrete.
6. EDS analysis showed higher amounts of strength-enhancing components such as $CaCO_3$, SiO_2, MgO, and Al_2O_3 in the FA20CNC0.2 mix.
7. The combined action of FA and CNC enhanced hydration, promoted pore filling, and strengthened the formation of C-S-H bonds.
8. This method decreases the amount of cement needed while improving the quality of concrete, presenting an environmentally friendly and sustainable option for producing high-performance concrete.

The integration of FA and CNC results in concrete that boasts enhanced mechanical characteristics and microstructure, while also minimizing the environmental footprint of cement production. This approach offers a viable path for creating sustainable, high-performance concrete suitable for construction purposes.

Acknowledgement

The authors wish to express the gratitude to UltraTech Cement Pvt. Ltd. for providing material support for the experimentation purpose. The assistance and encouragement from colleagues and friends are also gratefully acknowledged.

Conflict of Interest

Authors declare that there is no conflict of interests regarding the publication of the paper.

Author Contribution

The authors confirm contribution to the paper as follows: ***conceptualization:*** *Varsha More, Dr. S.S.Jamkar;* ***methodology:*** *Varsha More, Dr. S.S.Jamkar;* ***formal analysis and investigation:*** *Varsha More, Dr. S.S.Jamkar;* ***writing - original draft preparation:*** *Varsha More****; writing - review and editing:*** *Varsha More;* ***supervision:*** *Dr. S.A.Bhalchandra, Dr. S.S.Jamkar;* ***All authors reviewed the results and approved the final version of the manuscript.***

References

[1] L. Wang, P. Zhang, G. Golewski, and J. Guan, 'Editorial: Fabrication and properties of concrete containing industrial waste', *Front. Mater.*, vol. 10, p. 1169715, Mar. 2023, doi: 10.3389/fmats.2023.1169715.

[2] B. Tipraj, K. Athira, and T. Shanmuga Priya, 'Role of agro waste in geopolymer concrete: strength, durability and microstructural properties', *Eng. Res. Express*, vol. 7, no. 1, p. 015107, Mar. 2025, doi: 10.1088/2631-8695/ada7c6.

[3] A. M. Zeyad, M. Shubaili, N. B. Frahat, A. H. Khan, and I. S. Agwa, 'Evaluation of sustainable lightweight concrete incorporating popcorn and pumice aggregates with sugarcane leaf ash', *Sustainable Chemistry and Pharmacy*, vol. 45, p. 101975, Jun. 2025, doi: 10.1016/j.scp.2025.101975.

[4] Z. Lin, G. Lyu, and K. Fang, 'Carbon emissions assessment of concrete and quantitative calculation of CO2 reduction benefits of SCMs: A case study of C30-C80 ready-mixed concrete in China', *Case Studies in Construction Materials*, vol. 22, p. e04287, Jul. 2025, doi: 10.1016/j.cscm.2025.e04287.

[5] K. Moolchandani, 'Industrial byproducts in concrete: A state-of-the-art review', *Next Materials*, vol. 8, p. 100593, Jul. 2025, doi: 10.1016/j.nxmate.2025.100593.

[6] G. L. Golewski, 'Examination of water absorption of low volume fly ash concrete (LVFAC) under water immersion conditions', *Mater. Res. Express*, vol. 10, no. 8, p. 085505, Aug. 2023, doi: 10.1088/2053-1591/acedef.

[7] Q. Song *et al.*, 'Novel high-efficiency solid particle foam stabilizer: Effects of modified fly ash on foam properties and foam concrete', *Cement and Concrete Composites*, vol. 155, p. 105818, Jan. 2025, doi: 10.1016/j.cemconcomp.2024.105818.

[8] H. Zhang *et al.*, 'Optimization of low-carbon lightweight foamed concrete using ground circulating fluidized bed fly ash', *Journal of Cleaner Production*, vol. 489, p. 144697, Jan. 2025, doi: 10.1016/j.jclepro.2025.144697.

[9] M. Mathapati, K. Amate, C. Durga Prasad, M. L. Jayavardhana, and T. Hemanth Raju, 'A review on fly ash utilization', *Materials Today: Proceedings*, vol. 50, pp. 1535–1540, 2022, doi: 10.1016/j.matpr.2021.09.106.

[10] M. Z. M. Nomani, O. Shaquib, and M. Sharma, 'Fly Ash in Concrete Production: A Legal and Regulatory Review of Environmental Impacts', *Nat. Env. Poll. Tech*, vol. 24, no. S1, pp. 305–314, Jan. 2025, doi: 10.46488/NEPT.2024.v24iS1.023.

[11] S. S. Alterary and N. H. Marei, 'Fly ash properties, characterization, and applications: A review', *Journal of King Saud University - Science*, vol. 33, no. 6, p. 101536, Sep. 2021, doi: 10.1016/j.jksus.2021.101536.

[12] T. Fantu, G. Alemayehu, G. Kebede, Y. Abebe, S. K. Selvaraj, and V. Paramasivam, 'Experimental investigation of compressive strength for fly ash on high strength concrete C-55 grade', *Materials Today: Proceedings*, vol. 46, pp. 7507–7517, 2021, doi: 10.1016/j.matpr.2021.01.213.

[13] G. Golewski, 'The Beneficial Effect of the Addition of Fly Ash on Reduction of the Size of Microcracks in the ITZ of Concrete Composites under Dynamic Loading', *Energies*, vol. 14, no. 3, p. 668, Jan. 2021, doi: 10.3390/en14030668.

[14] L. S. Ho and T.-P. Huynh, 'Long-term mechanical properties and durability of high-strength concrete containing high-volume local fly ash as a partial cement substitution', *Results in Engineering*, vol. 18, p. 101113, Jun. 2023, doi: 10.1016/j.rineng.2023.101113.

[15] Y. Nie, J. Shi, Z. He, B. Zhang, Y. Peng, and J. Lu, 'Evaluation of high-volume fly ash (HVFA) concrete modified by metakaolin: Technical, economic and environmental analysis', *Powder Technology*, vol. 397, p. 117121, Jan. 2022, doi: 10.1016/j.powtec.2022.117121.

[16] G. L. Golewski, 'Enhancement fracture behavior of sustainable cementitious composites using synergy between fly ash (FA) and nanosilica (NS) in the assessment based on digital image processing procedure', *Theoretical and Applied Fracture Mechanics*, vol. 131, p. 104442, Jun. 2024, doi: 10.1016/j.tafmec.2024.104442.

[17] K. M. Elhadi, A. Raza, N. Ghazouani, and D. Khan, 'Physical properties and material characterisation of fly ash-based geopolymer composites having nano silica and micro glass', *European Journal of Environmental and Civil Engineering*, pp. 1–22, Mar. 2025, doi: 10.1080/19648189.2025.2474577.

[18] Q. Li, Y. Fan, Y. Zhao, H. Chen, and S. P. Shah, 'AC impedance spectroscopy interpretation of the hydration behavior for cement mortar containing fly ash and nano-metakaolin', *Construction and Building Materials*, vol. 468, p. 140436, Mar. 2025, doi: 10.1016/j.conbuildmat.2025.140436.

[19] M. A. Jamal, A. S. Mohammed, and J. A. Ali, 'Modeling the impact of SiO2, Al2O3, CaO, and Fe2O3 on the compressive strength of cement modified with nano-silica and silica fume', *Multiscale and Multidiscip. Model. Exp. and Des.*, vol. 8, no. 2, p. 156, Feb. 2025, doi: 10.1007/s41939-025-00739-w.

[20] G. L. Golewski, 'Determination of Fracture Mechanic Parameters of Concretes Based on Cement Matrix Enhanced by Fly Ash and Nano-Silica', *Materials*, vol. 17, no. 17, p. 4230, Aug. 2024, doi: 10.3390/ma17174230.

[21] S. Baran, A. Baran, S. N. Bicakci, H. N. Turkmenoglu, and H. N. Atahan, 'Fresh, Setting, and Hardened Properties of Fly Ash Concrete with Nano-Silica', *Arab J Sci Eng*, vol. 50, no. 3, pp. 1683–1702, Feb. 2025, doi: 10.1007/s13369-024-09022-5.

[22] G. Nassrullah *et al.*, 'Optimizing cement-based material formulation for 3D printing: Integrating carbon nanotubes and silica fume', *Case Studies in Construction Materials*, vol. 22, p. e04579, Jul. 2025, doi: 10.1016/j.cscm.2025.e04579.

[23] A. A. Raheem, R. Abdulwahab, and M. A. Kareem, 'Incorporation of metakaolin and nanosilica in blended cement mortar and concrete- A review', *Journal of Cleaner Production*, vol. 290, p. 125852, Mar. 2021, doi: 10.1016/j.jclepro.2021.125852.

[24] X. Wang, C. Gong, J. Lei, J. Dai, L. Lu, and X. Cheng, 'Effect of silica fume and nano-silica on hydration behavior and mechanism of high sulfate resistance Portland cement', *Construction and Building Materials*, vol. 279, p. 122481, Apr. 2021, doi: 10.1016/j.conbuildmat.2021.122481.

[25] K. Sobolev and M. F. Gutiérrez, 'Successfully mimicking nature's bottom-up construction processes is one of the most promising directions.', *American Ceramic Society Bulletin*, vol. 84, no. 10, 2005.

[26] M. Subhan, K. Choudhury, and N. Neogi, 'Advances with Molecular Nanomaterials in Industrial Manufacturing Applications', *Nanomanufacturing*, vol. 1, no. 2, pp. 75–97, Aug. 2021, doi: 10.3390/nanomanufacturing1020008.

[27] M. S. M. Norhasri, M. S. Hamidah, and A. M. Fadzil, 'Applications of using nano material in concrete: A review', *Construction and Building Materials*, vol. 133, pp. 91–97, Feb. 2017, doi: 10.1016/j.conbuildmat.2016.12.005.

[28] S. Chakraborty, B. W. Jo, and Y.-S. Yoon, 'Development of nano cement concrete by top-down and bottom-up nanotechnology concept', in *Smart Nanoconcretes and Cement-Based Materials*, Elsevier, 2020, pp. 183–213. doi: 10.1016/B978-0-12-817854-6.00007-6.

[29] H. Hamada, J. Shi, S. T. Yousif, M. Al Jawahery, B. Tayeh, and G. Jokhio, 'Use of nano-silica in cement-based materials – a comprehensive review', *Journal of Sustainable Cement-Based Materials*, vol. 12, no. 10, pp. 1286–1306, Oct. 2023, doi: 10.1080/21650373.2023.2214146.

[30] P. Aggarwal, R. P. Singh, and Y. Aggarwal, 'Use of nano-silica in cement based materials—A review', *Cogent Engineering*, vol. 2, no. 1, p. 1078018, Dec. 2015, doi: 10.1080/23311916.2015.1078018.

[31] H. Yang *et al.*, 'Effects of nano silica on the properties of cement-based materials: A comprehensive review', *Construction and Building Materials*, vol. 282, p. 122715, May 2021, doi: 10.1016/j.conbuildmat.2021.122715.

[32] S. Li *et al.*, 'The performance and functionalization of modified cementitious materials via nano titanium-dioxide: A review', *Case Studies in Construction Materials*, vol. 19, p. e02414, Dec. 2023, doi: 10.1016/j.cscm.2023.e02414.

[33] M. Ramezani, A. Dehghani, and M. M. Sherif, 'Carbon nanotube reinforced cementitious composites: A comprehensive review', *Construction and Building Materials*, vol. 315, p. 125100, Jan. 2022, doi: 10.1016/j.conbuildmat.2021.125100.

[34] T. V. Patil, D. K. Patel, S. D. Dutta, K. Ganguly, T. S. Santra, and K.-T. Lim, 'Nanocellulose, a versatile platform: From the delivery of active molecules to tissue engineering applications', *Bioactive Materials*, vol. 9, pp. 566–589, Mar. 2022, doi: 10.1016/j.bioactmat.2021.07.006.

[35] L. Perrin, G. Gillet, L. Gressin, and S. Desobry, 'Interest of Pickering Emulsions for Sustainable Micro/Nanocellulose in Food and Cosmetic Applications', *Polymers*, vol. 12, no. 10, p. 2385, Oct. 2020, doi: 10.3390/polym12102385.

[36] A. Balea, E. Fuente, A. Blanco, and C. Negro, 'Nanocelluloses: Natural-Based Materials for Fiber-Reinforced Cement Composites. A Critical Review', *Polymers*, vol. 11, no. 3, p. 518, Mar. 2019, doi: 10.3390/polym11030518.

[37] H. Withana, S. Rawat, and Y. X. Zhang, 'Effect of nanocellulose on mechanical properties of cementitious composites – A review', *Advanced Nanocomposites*, vol. 1, no. 1, pp. 201–216, 2024, doi: 10.1016/j.adna.2024.05.003.

[38] A. Guo, Z. Sun, N. Sathitsuksanoh, and H. Feng, 'A Review on the Application of Nanocellulose in Cementitious Materials', *Nanomaterials (Basel)*, vol. 10, no. 12, p. 2476, Dec. 2020, doi: 10.3390/nano10122476.

[39] M. Nasir *et al.*, 'Recent review on synthesis, evaluation, and SWOT analysis of nanostructured cellulose in construction applications', *Journal of Building Engineering*, vol. 46, p. 103747, Apr. 2022, doi: 10.1016/j.jobe.2021.103747.

[40] R. F. Santos *et al.*, 'Nanofibrillated cellulose and its applications in cement-based composites: A review', *Construction and Building Materials*, vol. 288, p. 123122, Jun. 2021, doi: 10.1016/j.conbuildmat.2021.123122.

[41] K. Dhali, M. Ghasemlou, F. Daver, P. Cass, and B. Adhikari, 'A review of nanocellulose as a new material towards environmental sustainability', *Science of The Total Environment*, vol. 775, p. 145871, Jun. 2021, doi: 10.1016/j.scitotenv.2021.145871.

[42] S. Ghahari, L. N. Assi, A. Alsalman, and K. E. Alyamaç, 'Fracture Properties Evaluation of Cellulose Nanocrystals Cement Paste', *Materials*, vol. 13, no. 11, p. 2507, May 2020, doi: 10.3390/ma13112507.

[43] H.-J. Lee and W. Kim, 'Long-term durability evaluation of fiber-reinforced ECC using wood-based cellulose nanocrystals', *Construction and Building Materials*, vol. 238, p. 117754, Mar. 2020, doi: 10.1016/j.conbuildmat.2019.117754.

[44] H. Feng *et al.*, 'Mechanical properties and microstructure of cellulose nanocrystal modified cement pastes subject to chloride erosion', *Journal of Building Engineering*, vol. 107, p. 112670, Aug. 2025, doi: 10.1016/j.jobe.2025.112670.

[45] G. Xu and X. Shi, 'Characteristics and applications of fly ash as a sustainable construction material: A state-of-the-art review', *Resources, Conservation and Recycling*, vol. 136, pp. 95–109, Sep. 2018, doi: 10.1016/j.resconrec.2018.04.010.

[46] A. N. Reddy, P. N. Reddy, B. V. Kavyateja, and G. G. K. Reddy, 'Influence of nanomaterial on high-volume fly ash concrete: a statistical approach', *Innov. Infrastruct. Solut.*, vol. 5, no. 3, p. 88, Dec. 2020, doi: 10.1007/s41062-020-00340-9.

[47] 'IS 456 (2000): Plain and Reinforced Concrete - Code of Practice'.

[48] 'IS-269-2015- ordinary portland cement specification'.

[49] 'IS 3812-1 (2033): Specification for Pulverized Fuel Ash, Part 1: For Use as Pozzolana in Cement, Cement Mortar and Concrete'.

[50] M. A. Aziz, M. Zubair, and M. Saleem, 'Development and testing of cellulose nanocrystal-based concrete', *Case Studies in Construction Materials*, vol. 15, p. e00761, Dec. 2021, doi: 10.1016/j.cscm.2021.e00761.

[51] H.-J. Lee, H.-S. Lee, J. Seo, Y.-H. Kang, W. Kim, and T. Kang, 'State-of-the-Art of Cellulose Nanocrystals and Optimal Method for their Dispersion for Construction-Related Applications', *Applied Sciences*, vol. 9, no. 3, p. 426, Jan. 2019, doi: 10.3390/app9030426.

[52] IS: 383-2016. Specification for Coarse and Fine Aggregates from Natural Sources for Concrete (Second Revision), Bureau of Indian Standards, Manak Bhavan, 9 Bahadur Shah Zafar Marg, New Delhi 110002

[53] Indian standards guidelines for design and development of different types of concrete mixes, IS 10262:2019. Bureau of Indian Standards, New Delhi.

[54] IS, X. (2006). 516-1959 "Indian Standard Methods of Tests for Strength of concrete". *Bureau of Indian Standards, New Delhi, India*.

[55] IS 5816-1999, Method of Test for Splitting Tensile Strength of Concrete., Bureau of Indian Standards, New Delhi, India.

[56] C. Rajesh and G. R. Kumar, 'A new shear test setup for determining shear strength of normal and high strength concrete', *Structures*, vol. 54, pp. 1046–1057, Aug. 2023, doi: 10.1016/j.istruc.2023.05.132.

[57] Q. Liu, Y. Peng, L. Liang, X. Dong, and H. Li, 'Effect of Cellulose Nanocrystals on the Properties of Cement Paste', *Journal of Nanomaterials*, vol. 2019, pp. 1–7, Dec. 2019, doi: 10.1155/2019/8318260.

[58] Y. M. Zhang, W. Sun, and H. D. Yan, 'Hydration of high-volume fly ash cement pastes', *Cement & Concrete Composites*, vol. 22, p. 445±452, 2000.

[59] S. Kang, Z. Lloyd, T. Kim, and M. T. Ley, 'Predicting the compressive strength of fly ash concrete with the Particle Model', *Cement and Concrete Research*, vol. 137, p. 106218, Nov. 2020, doi: 10.1016/j.cemconres.2020.106218.

[60] N. Yaseen, S. Alcivar-Bastidas, M. Irfan-ul-Hassan, D. M. Petroche, A. U. Qazi, and A. D. Ramirez, 'Concrete incorporating supplementary cementitious materials: Temporal evolution of compressive strength and environmental life cycle assessment', *Heliyon*, vol. 10, no. 3, p. e25056, Feb. 2024, doi: 10.1016/j.heliyon.2024.e25056.

[61] R. A. Hawileh, S. K. Shaw, M. Assad, A. Dey, J. A. Abdalla, and J. H. Kim, 'Influence of Fly Ash on the Compressive Strength of Ultrahigh-Performance Concrete: A State-of-the-art Review Towards Sustainability', *Int J Concr Struct Mater*, vol. 19, no. 1, p. 25, Apr. 2025, doi: 10.1186/s40069-024-00757-x.

[62] Y. Cao, P. Zavaterri, J. Youngblood, R. Moon, and J. Weiss, 'The influence of cellulose nanocrystal additions on the performance of cement paste', *Cement and Concrete Composites*, vol. 56, pp. 73–83, Feb. 2015, doi: 10.1016/j.cemconcomp.2014.11.008.

[63] J. Flores, M. Kamali, and A. Ghahremaninezhad, 'An Investigation into the Properties and Microstructure of Cement Mixtures Modified with Cellulose Nanocrystal', *Materials*, vol. 10, no. 5, p. 498, May 2017, doi: 10.3390/ma10050498.

[64] M. R. Dousti, Y. Boluk, and V. Bindiganavile, 'The effect of cellulose nanocrystal (CNC) particles on the porosity and strength development in oil well cement paste', *Construction and Building Materials*, vol. 205, pp. 456–462, Apr. 2019, doi: 10.1016/j.conbuildmat.2019.01.073.

[65] D. Zheng, H. Yang, W. Feng, Y. Fang, and H. Cui, 'Modification mechanism of cellulose nanocrystals in cement', *Cement and Concrete Research*, vol. 165, p. 107089, Mar. 2023, doi: 10.1016/j.cemconres.2023.107089.

[66] H. Feng, Y. Su, A. Guo, Z. Yu, and Z. Guo, 'Mechanical properties of cellulose nanocrystal modified cement/fly ash pastes under various water/binder ratios', *Construction and Building Materials*, vol. 447, p. 138213, Oct. 2024, doi: 10.1016/j.conbuildmat.2024.138213.

[67] Y. Cao, P. Zavaterri, J. Youngblood, R. Moon, and J. Weiss, 'The influence of cellulose nanocrystal additions on the performance of cement paste', *Cement and Concrete Composites*, vol. 56, pp. 73–83, Feb. 2015, doi: 10.1016/j.cemconcomp.2014.11.008.

[68] R. Jarabo, E. Fuente, J. L. García Calvo, P. Carballosa, and C. Negro, 'Nanocrystalline Cellulose to Reduce Superplasticizer Demand in 3D Printing of Cementitious Materials', *Materials*, vol. 17, no. 17, p. 4247, Aug. 2024, doi: 10.3390/ma17174247.

[69] T. Matschei, B. Lothenbach, and F. P. Glasser, 'The role of calcium carbonate in cement hydration', *Cement and Concrete Research*, vol. 37, no. 4, pp. 551–558, Apr. 2007, doi: 10.1016/j.cemconres.2006.10.013.

[70] S. Liu and P. Yan, 'Effect of limestone powder on microstructure of concrete', *J. Wuhan Univ. Technol.-Mat. Sci. Edit.*, vol. 25, no. 2, pp. 328–331, Apr. 2010, doi: 10.1007/s11595-010-2328-5.

[71] Y. Qing, Z. Zenan, K. Deyu, and C. Rongshen, 'Influence of nano-SiO2 addition on properties of hardened cement paste as compared with silica fume', *Construction and Building Materials*, vol. 21, no. 3, pp. 539–545, Mar. 2007, doi: 10.1016/j.conbuildmat.2005.09.001.

[72] X. Liu and Y. Li, 'Effect of MgO on the composition and properties of alite-sulphoaluminate cement', *Cement and Concrete Research*, vol. 35, no. 9, pp. 1685–1687, Sep. 2005, doi: 10.1016/j.cemconres.2004.08.008.

[73] M. Saliani, A. Honarbakhsh, R. Zhiani, S. M. Movahedifar, and A. Motavalizadehkakhky, 'Effects of GO/Al_2O_3 and Al_2O_3 Nanoparticles on Concrete Durability against High Temperature, Freeze-Thaw Cycles, and Acidic Environments', *Advances in Civil Engineering*, vol. 2021, no. 1, p. 4555802, Jan. 2021, doi: 10.1155/2021/4555802.

[74] A. P. B. Capraro, J. Hoppe Filho, and M. H. Medeiros, 'Influence of internal sulfate attack on cement paste properties: contamination by pyrite', *Rev. IBRACON Estrut. Mater.*, vol. 14, no. 6, p. e14606, 2021, doi: 10.1590/s1983-41952021000600006.